Desiccation of the resurrection plant *Craterostigma plantagineum* induces dynamic changes in protein phosphorylation

HORST RÖHRIG[1], JÜRGEN SCHMIDT[2], THOMAS COLBY[2], ANNE BRÄUTIGAM[2], PETER HUFNAGEL[3] & DOROTHEA BARTELS[1]

[1]*Institute of Molecular Physiology and Biotechnology of Plants (IMBIO), University of Bonn, Kirschallee 1, D-53115 Bonn, Germany,* [2]*Max Planck Institute for Plant Breeding, Carl-von-Linné-Weg 10, D-50829 Cologne, Germany and* [3]*Bruker Daltonics GmbH, Fahrenheitstr. 4, D-28359 Bremen, Germany*

ABSTRACT

Reversible phosphorylation of proteins is an important mechanism by which organisms regulate their reactions to external stimuli. To investigate the involvement of phosphorylation during acquisition of desiccation tolerance, we have analysed dehydration-induced protein phosphorylation in the desiccation tolerant resurrection plant *Craterostigma plantagineum*. Several dehydration-induced proteins were shown to be transiently phosphorylated during a dehydration and rehydration (RH) cycle. Two abundantly expressed phosphoproteins are the dehydration- and abscisic acid (ABA)-responsive protein CDeT11-24 and the group 2 late embryogenesis abundant (LEA) protein CDeT6-19. Although both proteins accumulate in leaves and roots with similar kinetics in response to dehydration, their phosphorylation patterns differ. Several phosphorylation sites were identified on the CDeT11-24 protein using liquid chromatography-tandem mass spectrometry (LC-MS/MS). The coincidence of phosphorylation sites with predicted coiled-coil regions leads to the hypothesis that CDeT11-24 phosphorylations influence the stability of coiled-coil interactions with itself and possibly other proteins.

Key-words: coiled-coil domains, desiccation tolerance; LEA proteins; phosphorylation site mapping.

INTRODUCTION

The integrity of cellular structures during severe water loss is a phenomenon in several biological systems which has not yet been understood. The South African anhydrobiotic plant *Craterostigma plantagineum* is used as an experimental system to study the molecular basis of desiccation tolerance (Bartels & Salamini 2001). This plant tolerates a loss of up to 98% of the cellular water, and desiccated plants remain viable for several months. After rehydration (RH),

Correspondence: Horst Röhrig. Fax: +49 228 73 1697; e-mail: hroehrig@uni-bonn.de

dried vegetative tissues regain full physiological activity within several hours (Gaff 1971). Nearly all flowering plants tolerate desiccation during seed formation, but most plants lose the ability to recover from complete dryness after germination, and thus desiccation tolerance is developmentally restricted.

Similar molecules seem to be involved in desiccation of seeds and vegetative leaves of resurrection plants (Bartels 2005). Considerable effort has been directed towards the identification of proteins which accumulate in vegetative tissues of *C. plantagineum* in response to dehydration (Bartels & Salamini 2001; Bartels & Sunkar 2005). These proteins can be classified into different functional groups (Bartels & Salamini 2001) and are likely to be involved in the acquisition of desiccation tolerance. The most abundant group of dehydration-induced proteins are the so called late embryogenesis abundant (LEA) proteins (Bartels & Salamini 2001). On the basis of sequence similarity, LEA proteins are grouped into several different classes, but they all share a high degree of hydrophilicity and the lack of cysteine residues (Cuming 1999. Although the biological function of LEA proteins is still unknown, they are correlated with dehydration in seeds or vegetative tissues (Cuming 1999; Bartels & Salamini 2001). It has been proposed that LEA proteins play an essential role in protecting cellular structures from the damaging effect of water loss (Wise & Tunnacliffe 2004; Reyes *et al.* 2005). The protective function has been supported by transgenic yeast and plants overexpressing LEA proteins and by *in vitro* protection assays (Bartels & Sunkar 2005). This protecting function can also be exerted by the LEA-like dehydrin gene from the moss *Physcomitrella* as shown by Saavedra *et al.* (2006). Possibly, a synergistic effect of LEA proteins and non-reducing disaccharides is necessary for protection, because disaccharides such as sucrose and trehalose are known to accumulate during dehydration and have been correlated with osmotic stress in plants and nematodes (Bartels & Sunkar 2005; Goyal, Walton & Tunnacliffe 2005).

The complex process of desiccation tolerance may not only involve the accumulation of a number of stress-related proteins, but may also require post-translational

modifications which could rapidly alter the biochemical properties of the proteins. Phosphorylation is an important post-translational modification of proteins. Reversible phosphorylation of Ser, Thr and Tyr residues is a modulator of protein function, and a mechanism by which organisms regulate processes in response to environmental stimuli (Huber & Hardin 2004; Pawson & Scott 2005). It has previously been shown that the LEA-like protein CAP160 from spinach is a phosphoprotein (Guy & Haskell 1989) and that the maize dehydrin Rab17 is the most heavily phosphorylated protein in mature embryos (Goday *et al*. 1988). Transcriptome analyses have shown that several classes of protein kinases and phosphatases are up-regulated during dehydration stress which indicates that reversible phosphorylation processes are frequent reactions during dehydration (Bartels & Sunkar 2005).

To investigate whether phosphorylation is involved in acquisition of desiccation tolerance, we have monitored dehydration-induced protein phosphorylation in *C. plantagineum* during a dehydration/RH cycle. The analysis was performed with leaves and roots because these tissues differ in their responses to water availability (Bartels & Salamini 2001). Two groups of proteins which were transiently phosphorylated upon dehydration stress were identified as the dehydration- and abscisic acid (ABA)-responsive protein CDeT11-24 (Velasco, Salamini & Bartels 1998) and the group 2 LEA protein CDeT6-19 (Schneider *et al*. 1993). Both proteins are encoded by small multigene families and accumulate abundantly in response to dehydration. We propose a model that phosphorylation of CDeT11-24 may be important in interactions with other cellular structures.

MATERIALS AND METHODS

Plant material and growth conditions

Craterostigma plantagineum Hochst. plants were propagated vegetatively and were grown in a growth chamber (light period of 16 h, light intensity 4000 lx, day/night temperature of 23/19 °C, 50% relative humidity) in individual pots with artificial substrate (Seramis; Masterfoods GmbH, Verden, Germany). The plants were always kept fully watered with 0.1% (v/v) Wuxal (Bayer, Langenfeld, Germany). To dry the *C. plantagineum* plants, watering was withdrawn, and the plants were kept under normal growth conditions for several days. The relative water content (RWC) was used to monitor the extent of water loss (Bernacchia *et al*. 1995). For RH, desiccated plants were fully submerged in water for 24 h (RH1d) and then cultivated under normal conditions for 2, 4 and 8 d (RH2, 4, 8).

Extraction of plant proteins

A total protein fraction was isolated using a phenol-based procedure according to Wang *et al*. (2003) with some modifications. Leaves and roots were pooled from several plants and ground to a fine powder under liquid nitrogen.

Depending on the RWC of the plant tissues, 0.02 g (for plant material with 2% RWC) to 0.2 g (plant material with a RWC of 100%) of ground powder was transferred to 1.5 mL microtubes and resuspended in 1 mL of cold acetone. After vortexing for 30 s, the suspension was centrifuged (10 000 *g*, 5 min, 4 °C); the resulting pellet was washed once again with acetone and resuspended in 1 mL 10% (w/v) trichloroacetic acid (TCA) in acetone. The suspension was sonified in a sonication water bath for 10 min. After centrifugation, the pellets were sequentially washed twice with 10% (w/v) TCA in acetone, once with 10% (w/v) TCA and finally twice with 80% (v/v) acetone. This pellet was air-dried and the dry powder was resuspended in 0.7 mL 'dense sodium dodecyl sulphate (SDS)' buffer [30% (w/v) sucrose, 2% (w/v) SDS, 0.1 M tris(hydroxymethyl)aminomethane (Tris) -HCl pH 8.0, 5% (v/v) 2-mercaptoethanol]. Then 0.7 mL Tris-buffered phenol, pH 8.0 (Biomol, Hamburg, Germany) was added, and the resulting mixture was vortexed for 30 s. The phenol phase was separated by centrifugation and transferred to a fresh microtube. After addition of five volumes of cold 0.1 M ammonium acetate in methanol, the proteins were precipitated from the phenol phase for 30 min at −20 °C. The precipitated proteins were recovered by centrifugation, washed twice with cold 0.1 M ammonium actetate in methanol and twice with 80% (v/v) acetone. The final pellet was dried and stored at −80 °C. A separately precipitated aliquot was dissolved in a small volume of 8 M urea for protein quantification using the Bradford assay (Bio-Rad, München, Germany) with bovine serum albumin (BSA) as standard. The described procedure was scaled up for preparative purposes.

Gel electrophoresis

Proteins were analysed by one- or two-dimensional polyacrylamide gel electrophoresis (PAGE). For one-dimensional gel electrophoresis, the samples were dissolved in NuPAGE sample buffer (Invitrogen, Karlsruhe, Germany), heated for 20 min at 70 °C, and the proteins were separated on NuPAGE 4–12% Bis(2-hydroxyethyl)imino (Bis)-Tris gels with 2-(N-morpholino)ethansulfonic acid (MES) -SDS running buffer (Invitrogen). Two-dimensional PAGE was performed using an Ettan IPGphor II isoelectric focussing (IEF) system (GE Healthcare, Freiburg, Germany) for the first dimension. The proteins (5–20 μg) were solubilized in 125 μL RH solution [7 M urea, 2 M thiourea, 2% (w/v) 3-[(3-cholamidopropyl)dimethyl-ammonio]-1-propanesulfonate (CHAPS), 0.2% (w/v) dithiothreitol (DTT), 0.5% (v/v) immobilized pH gradient (IPG) buffer pH 3–10, 0.002% (w/v) bromophenol blue] for at least 1 h at room temperature. For the isolelectric focussing, 7 cm IPG strips, pH 3–10 (GE Healthcare) were used. The strips were rehydrated for 14 h at 20 °C in rehydration solution, and IEF was conducted using the following voltage steps: 30 min at 500 V, 30 min at 1000 V and finally, 100 min at 5000 V. For the second dimension, 10% SDS-polyacrylamide gels (Laemmli 1970) or NuPAGE 4–12% Bis-Tris

ZOOM gels (Invitrogen) were used. IPG strips were prepared for the second dimension SDS-polyacrylamide gel by equilibrating them 15 min in equilibration buffer [50 mM Tris-HCl, pH 6.8, 6 M urea, 30% (v/v) glycerol, 2% SDS, 0.002% (w/v) bromphenol blue] supplemented with 1% (w/v) DTT, followed by equilibration for 15 min in equilibration buffer containing 2.5% (w/v) iodoacetamide. The strips used for electrophoresis on NuPAGE gels (Invitrogen) were incubated in the NuPAGE sample buffer (Invitrogen) with NuPAGE sample reducing agent (15 min) followed by NuPAGE sample buffer containing 2% (w/v) iodoacetamide.

Staining of gels

Phosphoproteins were stained with the Pro-Q Diamond fluorescent gel stain according to the protocol of the manufacturer (Invitrogen). After staining with Pro-Q Diamond, the gels were stained with total-protein fluorescent gel stain SYPRO Ruby (Invitrogen) to monitor whether equal amounts of protein were loaded onto the gels. The proteins stained with fluorescent dyes were visualized using a Typhoon 9200 scanner (GE Healthcare) at an excitation wavelength of 532 nm and a bandpass emission filter of 610 nm. Two-dimensional gels used for mass spectrometry (MS) analysis were stained with colloidal Coomassie (Invitrogen).

Immunoblot analysis and immunoprecipitation

Proteins separated on one- or two-dimensional gels were transferred to nitrocellulose membranes as described (Towbin, Staehelin & Gordon 1979). CDeT11-24 and CDeT6-19 proteins were detected using polyclonal antisera at a dilution of 1:5000 and 1:1000, respectively (Schneider *et al*. 1993; Velasco *et al*. 1998). Immunoprecipitations were performed as described (John *et al*. 1985) with modifications. In brief, leaf and root tissues were ground to a fine powder under liquid nitrogen, and 20 mg (for plant material with 2% RWC) or 100 mg (plant material with 100% RWC) of fine powdered tissue were dissolved in 200 μL lysis buffer [50 mM Tris-HCl, pH 8.0, 1% (w/v) SDS, 1 mM ethylenediamine tetraacetic acid (EDTA) and heated for 5 min at 100 °C. After cooling, the sample was diluted 1:10 with cold wash buffer 1 [50 mM Tris-HCl, pH 7.5, 150 mM NaCl, 0.1% (v/v) Nonidet P-40, 0.05% (w/v) sodium deoxycholate, 1 mM EDTA] and centrifuged for 10 min at 20 000 g. The clear supernatant was incubated with 50 μL of a homogeneous protein A-agarose suspension (Roche, Mannheim, Germany) for 2 h at 4 °C on a rocking platform to remove non-specific adsorption to protein A-agarose. Beads were pelleted by centrifugation (20 s, 12 000 g) and discarded. Two microlitres of polyclonal anti-CDeT11-24 serum or 5 μL of anti-CDeT6-19 serum was added to the supernatant, and the mixtures were incubated at 4 °C for 1 h on a rocking platform. The mixtures were incubated for 3 h with 50 μL of protein A-agarose suspension, before the beads were pelleted (20 s, 12 000 g, 4 °C). The resulting supernatant was

discarded. The pellets were washed twice (10 min, 4 °C) with 1 mL wash buffer 1, twice with 1 mL wash buffer 2 [50 mM Tris-HCl, pH 7.5, 500 mM NaCl, 0.1% (v/v) Nonidet P-40, 0.05% (w/v) sodium deoxycholate] and finally, once with wash buffer 3 [10 mM Tris-HCl, pH 7.5, 0.1% (v/v) Nonidet P-40, 0.05% (w/v) sodium deoxycholate]. After the final wash, the agarose bead pellet was resuspended in 50 μL NuPAGE sample buffer (Invitrogen), and bound complexes were released by heat treatment (20 min at 70 °C). Proteins were separated on NuPAGE 4–12% Bis-Tris gels which were stained with Pro-Q Diamond fluorescent gel stain (Invitrogen) to visualize CDeT11-24 and CDeT6-19 proteins.

Calf intestinal alkaline phosphatase (CIP) treatment

For the dephosphorylation reaction, 40 μg of denatured proteins, extracted from roots and leaves of desiccated plants, were resuspended in 100 μL 50 mM NH$_4$HCO$_3$ containing protease inhibitors (complete, EDTA free; Roche). After solubilization of the hydrophilic proteins in a sonication water bath (10 min) and subsequent centrifugation (5 min at 20 000 g), the supernatant was incubated with 17 U CIP (Roche) for 30 min at 30 °C. The resulting reaction mixtures were lyophilized and analysed by two-dimensional gel electrophoresis.

Enrichment of hydrophilic phosphoproteins

The hydrophilic proteins were solubilized from phenol-extracted proteins as follows. The denatured proteins (approximately 10 mg) were resuspended in 5 mL phosphoprotein lysis buffer containing 0.25% (w/v) CHAPS (Qiagen, Hilden, Germany), and the suspension was sonified for 10 min. Insoluble proteins were pelleted by centrifugation (10 000 g for 20 min at 4 °C), and the protein concentration of the supernatant was determined using the Bradford assay (Bio-Rad). Typically, 20–25% of the proteins were resolubilized from the total proteins isolated from fully desiccated plant tissues. These preparations were used to enrich phosphoproteins by affinity capture chromatography (phosphoprotein purification kit; Qiagen). A volume of the supernatant, containing 2.5 mg of proteins, was adjusted to a concentration of 0.1 mg mL^{-1} by adding the phosphoprotein lysis buffer with 0.25% (w/v) CHAPS, and the enrichment of phosphoproteins was performed according to the manufacturer's instructions using the phosphoprotein affinity columns. Eluted phosphoproteins were concentrated by ultrafiltration, and the elution buffer was exchanged against 50 mM NH$_4$HCO$_3$. The protein samples were lyophilized and analysed by one or two-dimensional gel electrophoresis. The final yield of phosphoproteins varied between 100 and 220 μg from one column.

Ms

Protein bands were excised from colloidal Coomassie blue-stained gels and digested in-gel with 250 ng trypsin

overnight at 37 °C (Shevchenko *et al.* 1996). The extracted peptides were desalted and concentrated for MALDI analyses using C18 ZipTips (Millipore, Schwalbach, Germany). Samples were mixed with equal volumes of a saturated solution of alpha-cyano-4-hydroxy-cinnamic acid (HCCA, Bruker Daltonics, Bremen, Germany) in 50% (v/v) acetonitrile/0.1% (v/v) trifluoroacetic acid (TFA). Mass spectra of tryptic peptides were taken with a Reflex IV matrix-assisted laser desorption ionization – time of flight (MALDI-TOF) MS (Bruker Daltonics). The peptide mass fingerprints (PMFs) obtained were processed in Xmass 5.1.16 (Bruker Daltonics) and were used to identify the corresponding proteins in the ProteinScape 1.2 database system (Bruker Daltonics) via Mascot searches (Matrix Science, London, UK).

For phosphorylation site mapping by liquid chromatography-tandem mass spectrometry (LC-MS/MS), residual organic solvent was removed from selected tryptic digests by vacuum centrifugation before liquid chromatography (LC) separation. Some samples underwent an additional step of phosphopeptide enrichment via Fe^{3+}-immobilized metal ion affinity chromatography (IMAC) (ZipTipMC, Millipore) following a slightly modified version of the manufacturer's instructions. The first elution step was performed using a 50 mM sodium phosphate pH 7.3, 200 mM NaCl solution before elution with 0.3 M ammonium hydroxide. Phosphopeptides were observed in both elutions. LC-MS/MS runs were performed on two different systems. Firstly, the peptides were separated via nano-LC with an Agilent G2226 nanoPump and G1389 microAutosampler equipped with a 100 μm, 20 mm, Biosphere C18 trapping column and a 75 μm, 150 mm, Biosphere C18 analytical column (NanoSeparations, Nieuwkoop, the Netherlands). These samples were analysed with a high-capacity trap (HCTultra) ion trap mass spectrometer (Bruker Daltonics). Secondly, the phosphopeptide-enriched samples were run on a CapLC system equipped with a NanoEase Symmetry C18 trapping column and a 75 μm, 150 mm Atlantis C18 analytical column coupled to a Q-ToFII spectrometer (Waters, Eschborn, Germany).

The phosphopeptides were identified on the basis of neutral loss behaviour (loss of phosphoric acid with a molecular weight of 97.98 Da) and subsequently fragmented using Phosphoscan (Bruker Daltonics) or parent ion discovery (PID) methodology in Masslynx 4.0 (Waters). Fragmentation [tandem mass spectrometry (MS/MS)] data were analysed with Mascot (Matrix Science) and examined visually to pinpoint the phosphorylation sites.

RESULTS

Desiccation of *C. plantagineum* induces phosphorylation of stress proteins

Total proteins were extracted from leaves and roots of untreated and fully dehydrated *C. plantagineum* plants and analysed by two-dimensional PAGE. Phosphoproteins were stained with Pro-Q Diamond fluorescent dye (Invitrogen), which detects phosphate groups attached to Ser,

Thr and Tyr residues (Fig. 1). The same gels were subsequently stained with the total protein fluorescent stain SYPRO Ruby (Invitrogen) to visualize total proteins and to check equal protein loading. Figure 1a and b show that dehydration induces phosphorylation of different proteins in leaves and roots. Strong signals for phosphoproteins were detected in two areas of the gels (labelled 1 and 2 in Fig. 1). To identify the corresponding phosphoproteins, spots were excised from the gels and subjected to in-gel tryptic digestions. The resulting peptides were identified by MALDI-TOF MS. The PMFs obtained were used to screen the National Center for Biotechnology Information database using the ProteinScape software (Bruker Daltonics) that triggered Mascot (Matrix Science) searches. The programme consistently identified the dehydration and ABA-responsive protein CDeT11-24 (Velasco *et al.* 1998) and the group 2 LEA protein CDeT6-19 (Schneider *et al.* 1993) in leaves and roots (Fig. 1a & b, spots 1 and 2, respectively). CDeT11-24 was identified in leaves and roots with sequence coverages of 53 and 44%, respectively, and the average deviations of the measured peptide masses compared with the theoretical values of CDeT11-24 peptides (GI 2644964) were less than 0.03 Da. Sequence coverages of 39 and 32% and average deviations of the measured peptide masses compared with the theoretical values of 0.07 Da have been obtained for CDeT6-19 peptides (GI 6138749) of the protein from leaves and roots, respectively.

Both proteins are very hydrophilic, and the migration rate of CDeT6-19 in the second dimension confirmed the predicted molecular mass of 16 kDa. However, the molecular mass of the CDeT11-24 protein (approximately 60 kDa) differs from the molecular mass predicted from the cDNA clones (43.2, 44.4 and 44.5 kDa). The unusual migration behaviour of CDeT11-24 on the denaturing PAGE could be due to the hydrophilicity of the protein and has already been described (Velasco *et al.* 1998).

Transient phosphorylation of CDeT11-24 and CDeT6-19 occurs with different kinetics

To analyse the kinetics of protein phosphorylation during a dehydration and RH cycle, proteins from leaves and roots of *C. plantagineum* plants, which had been dehydrated to different degrees, were separated by PAGE and visualized with the Pro-Q Diamond fluorescent dye (Invitrogen) (Fig. 2a & e). To validate the specificity of the phosphoprotein gel stain, ovalbumin (OVA, carrying two phosphate groups) and BSA (no phosphate group) were applied to the gels. A comparison of lanes 1 and 2 in Fig. 2a and e with the same lanes in Fig. 2c and f shows that the Pro-Q Diamond fluorescent dye (Invitrogen) specifically detects phosphoproteins. Phosphoproteins corresponding to CDeT11-24 and CDeT6-19 were identified by immunoprecipitation and immunoblot analysis (Fig. 2b, d & g). The immunoblot analyses revealed that both proteins accumulated very early at the onset of dehydration stress, when about 10% of the cellular water was lost (Fig. 2d & g, lanes 4). In the leaves, both proteins were no longer detected 4 d
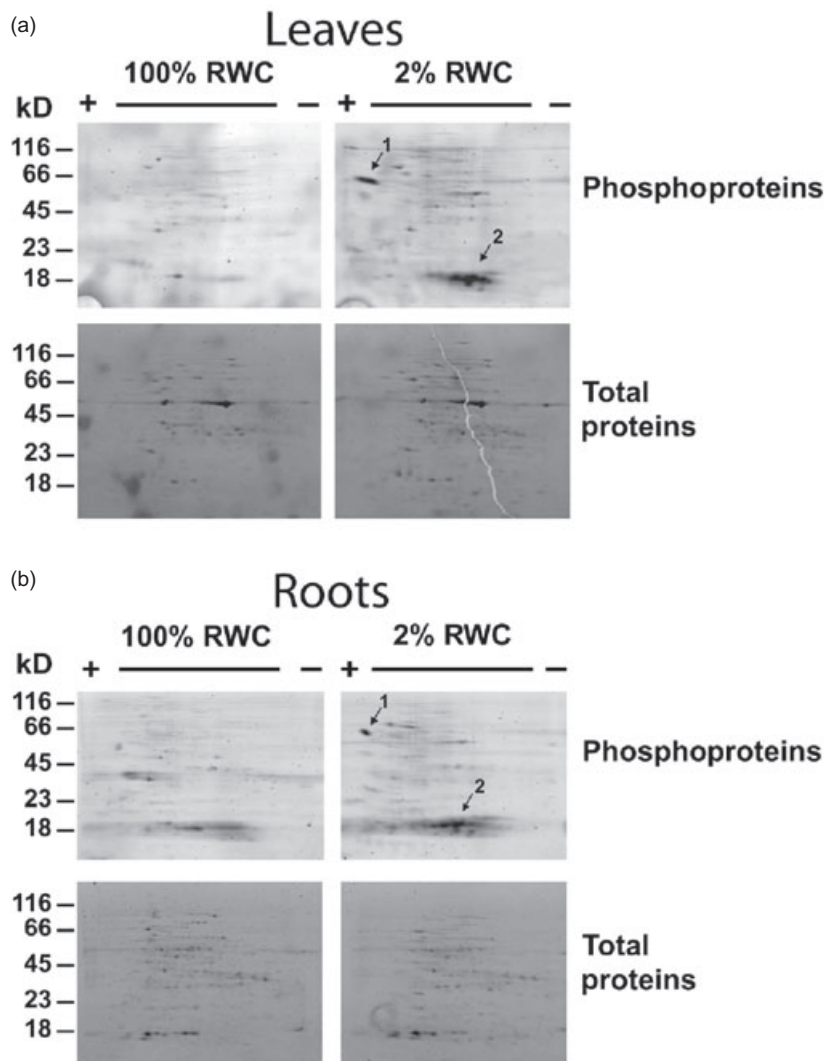
(a)

(b)

Figure 1. Monitoring desiccation-induced phosphoprotein accumulation by two-dimensional polyacrylamide gel electrophoresis (PAGE). Total proteins were isolated from leaves (a) and roots (b) of fully turgescent *Craterostigma plantagineum* plants [100% relative water content (RWC)] and desiccated plants (2% RWC), and 5 μg were loaded on each isoelectric focussing gel. Separation in the first dimension was performed by isoelectric focussing over the pH range 3–10 ((+), acidic pH; (−), basic pH) and in the second dimension on NuPAGE (Invitrogen, Karlsruhe, Germany) 4–12% bis(2-hydroxyethyl)imino-tris(hydroxymethyl)aminomethane (Bis-Tris) gels. Gels were stained with Pro-Q Diamond fluorescent gel stain (Invitrogen) to detect phosphoproteins, and subsequently with SYPRO Ruby (Invitrogen) to visualize the total proteins. Spots corresponding to CDeT11-24 (1) and CDeT6-19 (2) are indicated by black arrows.

after rewatering (Fig. 2d, lane 9), whereas the protein levels remain unchanged in the roots for a longer time (Fig. 2g). A comparison of the immunoblot analyses (Fig. 2d & g) with the corresponding phosphoprotein staining patterns (Fig. 2a & e) indicates that the kinetics of phosphorylation dynamics differs between CDeT11-24 and CDeT6-19. Extensive phosphorylation of CDeT6-19 was detected in all samples analysed. Protein accumulation and increase of phosphorylation are directly correlated (compare lanes 4–8 of Fig. 2a with the same lanes in Fig. 2d, and lanes 4–10 in Fig. 2e with Fig. 2g), indicating that phosphorylation takes place soon after dehydration-induced synthesis of the protein. However, the CDeT11-24 protein seems to get phosphorylated during late stages of dehydration at the transition of 40% RWC to complete dryness (2% RWC), and the phosphoprotein signal decreases already 1 d after rewatering (lanes 6 in Fig. 2a & e).

The phosphorylation of CDeT11-24 and CDeT6-19 was further analysed by comparative two-dimensional immuno-blot analyses. Polyclonal antisera were used to analyse the distribution of the proteins on the immunoblots. Figure 3a shows that the antibodies recognized CDeT11-24 proteins in leaves and roots of plants with 80, 40 and 2% RWCs, respectively. The distribution of the CDeT11-24 protein isolated from fully dehydrated plants (2% RWC) shifts during IEF to a more acidic pH compared with the protein pattern in partially dehydrated plants (80 and 40% RWC). This supports the previous finding that phosphorylated isoforms of this protein are more abundant in the fully desiccated tissues, but phosphorylation is hardly detectable in partially dehydrated tissues, although the protein is present. No shift was observed for the the CDeT6-19 spots (Fig. 3b) which is consistent with the finding that the protein is directly phosphorylated during synthesis as also shown in Fig. 2.

The phosphorylation of CDeT11-24 and CDeT6-19 was further confirmed by treatment of the proteins with CIP (Fig. 3c & d). Both proteins were resuspended from phenol-extracted proteins of desiccated plants, treated with CIP and analysed by two-dimensional immunoblot analysis. Figure 3c and d show that the phosphorylation-induced shift of CDeT11-24 (Fig. 3c) and CDeT6-19 (Fig. 3d) proteins to acidic pH is reversed by CIP treatment. The effect
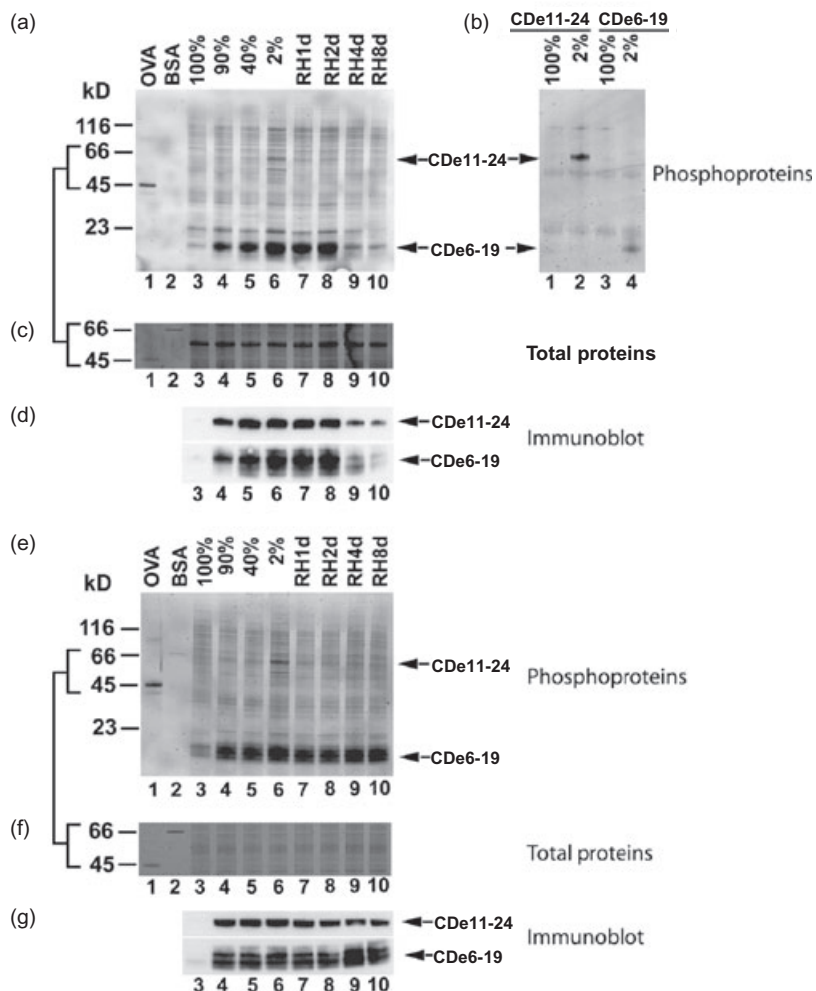
Figure 2. Transient phosphoprotein accumulation during dehydration and rehydration (RH) of *Craterostigma plantagineum* plants (a–d, leaves; e–g, roots). (a, e) Total proteins (lanes 3–10: 1 μg each lane) isolated from leaves (a) or roots (e) were separated on NuPAGE (Invitrogen, Karlsruhe, Germany) 4–12% bis(2-hydroxyethyl)imino-tris(hydroxymethyl)aminomethane (Bis-Tris) gels, and phosphoproteins were visualized with Pro-Q Diamond fluorescent (Invitrogen) gel stain. The relative water content (RWC) (lanes 3–6: 100, 90, 40 and 2%) and days of RH [lanes 7–10: 24 h (RH1d), 2 d (RH2d), 4 d (RH4d) and 8 d (RH8d)] of the plant material are indicated. Sizes of molecular mass markers are indicated on the left hand side. The specificity of the phosphoprotein staining was checked by applying ovalbumin (OVA) (lane 1: 50 ng OVA) and bovine serum albumin (BSA) (lane 2: 50 ng BSA) to the gels. (c, f) Parts of the gels shown in (a) and (e), which were subsequently stained for total proteins with SYPRO Ruby (Invitrogen) gel stain. (b) Immunoprecipitation of CDeT11-24 (lanes 1, 2) and CDeT6–19 (lanes 3, 4) from fully hydrated (100% RWC; lanes 1, 3) and desiccated (2% RWC; lanes 2, 4) leaf tissue; the gel was stained for phosphoproteins with Pro-Q Diamond dye (Invitrogen). (d, g) Immunoblot analysis of corresponding protein samples (lanes 3–10: 5 μg each lane) shown in (a) and (e), respectively. Proteins from leaves (d) and roots (g) were separated on NuPAGE gels (Invitrogen) and transferred to membranes. Polyclonal antisera raised against CDeT11-24 and CDeT6-19 were used to detect the corresponding proteins.

is more pronounced for the CDeT6-19 protein (Fig. 3d), indicating that this protein carries more phosphate groups than CDeT11-24.

Identification of phosphorylation sites in CDeT11-24

Next, we performed phosphorylation site mapping of CDeT11-24 by MS. To raise the sensitivity of the analysis, the phosphoproteins were enriched using affinity chromatography columns, which have already been shown to be effective for the enrichment of phosphoproteins from yeast (Metodiev, Timanova & Stone 2004; Makrantoni *et al.* 2005). Resolubilized proteins from leaves and roots of desiccated *C. plantagineum* plants (R, lanes 1 and 4 in Fig. 4) were applied to phosphoprotein affinity columns. Flow-through (Ft) and eluted fractions (Ef) were collected and analysed by gel electrophoresis. Figure 4a shows that very few phosphoproteins were obtained in the Ft, whereas most phosphoproteins were retained on the column and detected in the Ef. However, post staining of the gel with SYPRO Ruby (Invitrogen) for total proteins indicated that CDeT11-24 proteins are also present in the Ft (Fig. 4b).

This indicates that this protein is present as a mixture of phosphorylated and non-phosphorylated isoforms in desiccated tissues. In addition, MALDI-TOF analyses performed on immunoaffinity-purified whole protein indicated that the majority of phosphorylated CDeT11-24 carries a single phosphorylation (data not shown).

Enriched phosphoproteins were desalted, lyophilized and separated by two-dimensional gel electrophoresis. LC-MS/MS analysis of phosphopeptide-enriched tryptic digests of gel spots corresponding to CDeT11-24 with the CapLC/Q-ToFII (Waters) yielded two phosphopeptides with mass-to-charge ratios (m/z) of 834.32 (1+) and 683.78 (2+), representing the phosphorylated forms of tryptic peptides T30 and T29-30 from CDeT11-24 (Fig. 5b). Though fragmentation was weak, the observed ions indicated that Ser341 was the site of phosphorylation. These observations were confirmed and additional phosphopeptides were found by analysis with an HCTultra ion trap mass spectrometer (Bruker Daltonics). The phosphopeptides are listed in Fig. 5b. They were identified for CDeT11-24 from desiccated leaves and roots with the ion trap on the basis of the following criteria: (1) their masses correspond to those predicted for phosphorylated tryptic peptides from
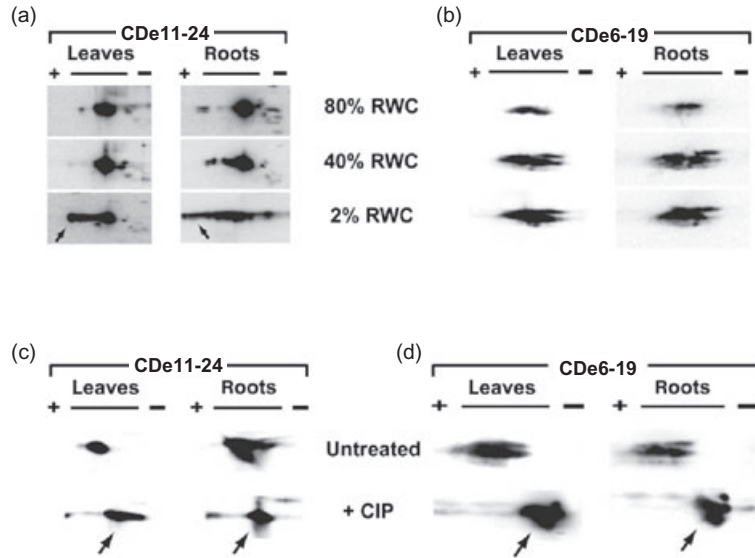
Figure 3. Comparative two-dimensional immunoblot analysis of CDeT11-24 and CDeT6-19. (a, b) Total proteins were isolated from leaves and roots of *Craterostigma plantagineum* plants during dehydration [relative water content (RWC) of 80, 40 or 2%]. The proteins were separated by two-dimensional gel electrophoresis (20 μg protein per gel) and transferred to nylon membranes. Separation in the second dimension was performed on 10% sodium dodecyl sulphate–polyacrylamide gel electrophoresis (SDS–PAGE) (a, c) or on NuPAGE (Invitrogen, Karlsruhe, Germany) 4–12% Bis-Tris gels (b, d). (a) Enlarged parts of the immunoblots showing CDeT11-24. (b) Parts of the immunoblots showing CDeT6-19. (c, d) Two-dimensional immunoblot analysis of calf intestinal alkaline phosphatase (CIP)-treated CDeT11-24 (c) and CDeT6-19 (d) proteins. Proteins extracted from leaves and roots of desiccated plants were treated with CIP for 30 min at 30 °C. Polyclonal antisera raised against CDeT11-24 (a, c) and CDeT6-19 (b, d) were used to detect the corresponding proteins. The positive (acidic end) and negative (basic end) polarity of the isoelectric focussing (IEF) are indicated by (+) and (–). Arrows indicate the shift of the CDeT11-24 and CDeT6-19 protein spots.

CDeT11-24; (2) they underwent a neutral loss of 97.98 Da (phosphoric acid) under low-energy fragmentation; and (3) microsequence information from full fragmentation matched the predicted tryptic fragments. The non-phosphorylated versions of all phosphopeptides were also observed in the samples analysed. Together, these results are consistent with multiple independent partial phosphorylations of the CDeT11-24. In Fig. 5a, the observed phosphorylation sites are indicated in the sequence of CDeT11-24.

In most cases, one phosphorylation site model best explained all fragmentation spectra for a given m/z. These sites are marked in green in Fig. 5a. A few MS/MS spectra for the phosphorylated T15, however, were best fit by

alternative models, shown in red (Fig. 5a). They may represent T15 peptides that were phosphorylated at other sites which cannot be chromatographically resolved from the major mode, or they may be artefacts of fitting to noisy spectra. The observation of a weak signal for a triply phosphorylated T15 peptide supports the multiple site hypothesis. The phosphorylation site on the T16 peptide (Ser169) is also uncertain because of noise in the spectrum. All CDeT11-24 phosphorylation sites observed with high certainty were also predicted on the basis of phosphorylation site models from either group-based phosphorylation scoring (GPS) (Fengfeng *et al*. 2004) or Prosite (version 19.14, http://www.expasy.org/prosite/).
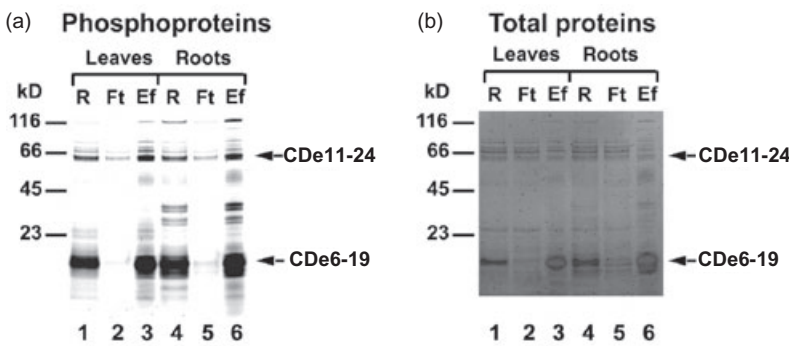

Figure 4. Enrichment of hydrophilic phosphoproteins using affinity chromatography. Resolubilized proteins (R) from leaves and roots of desiccated *Craterostigma plantagineum* plants were applied to phosphoprotein affinity columns and the flow-through (Ft) and eluted fractions (Ef) were collected. Phosphoproteins were separated on NuPAGE gels (Invitrogen, Karlsruhe, Germany) (1 μg per lane) and visualized with Pro-Q Diamond (Invitrogen) fluorescent stain (a) and subsequently with SYPRO Ruby (Invitrogen) (b). The CDeT11-24 and CDeT6-19 proteins are indicated.
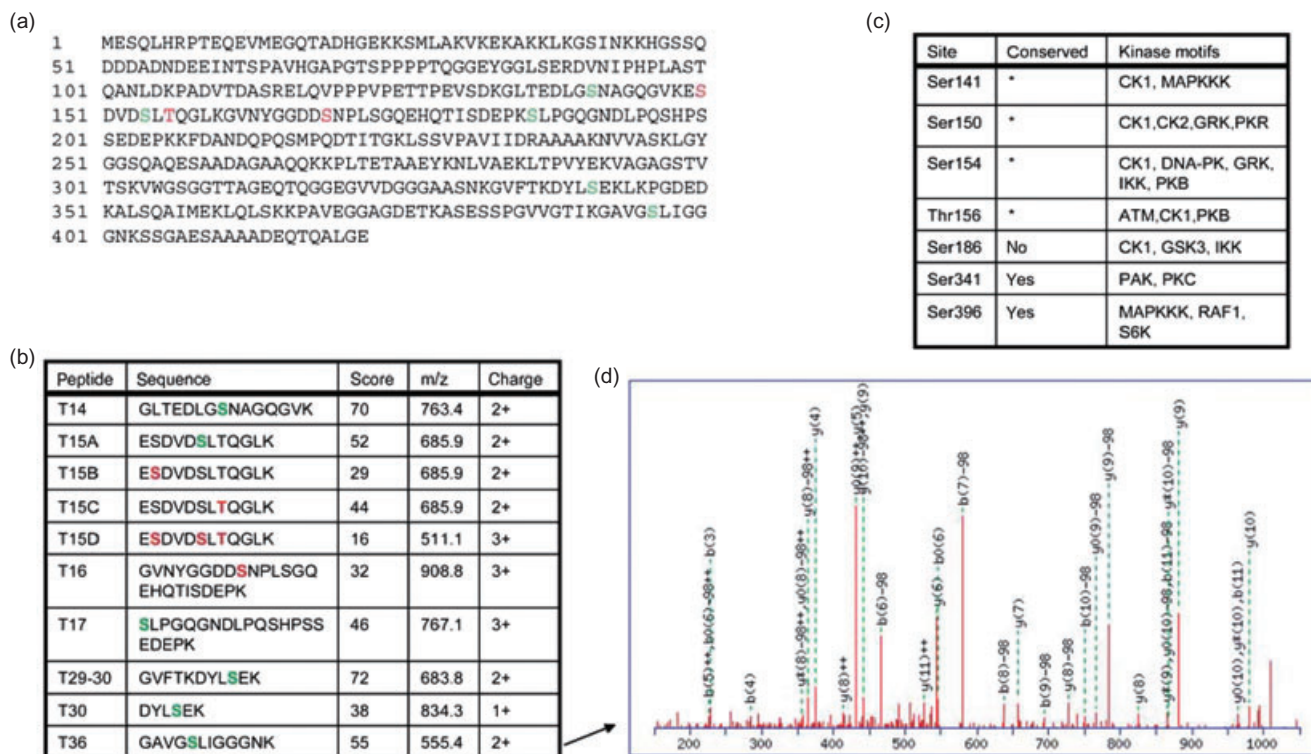
(a)

```
  1  MESQLHRPTEQEVMEGQTADHGEKKSMLAKVKEKAKKLKGSINKKHGSSQ
 51  DDDADNDEEINTSPAVHGAPGTSPPPPTQGGEYGGLSERDVNIPHPLAST
101  QANLDKPADVTDASRELQVPPPVPETTPEVSDKGLTEDLGSNAGQGVKES
151  DVDSLTQGLKGVNYGGDDSNPLSGQEHQTISDEPKSLPGQGNDLPQSHPS
201  SEDEPKKFDANDQPQSMPQDTITGKLSSVPAVIIDRAAAAKNVVASKLGY
251  GGSQAQESAADAGAAQQKKPLTETAAEYKNLVAEKLTPVYEKVAGAGSTV
301  TSKVWGSGGTTAGEQTQGGEGVVDGGGAASNKGVFTKDYLSEKLKPGDED
351  KALSQAIMEKLQLSKKPAVEGGAGDETKASESSPGVVGTIKGAVGSLIGG
401  GNKSSGAESAAAADEQTQALGE
```

(c)

Site	Conserved	Kinase motifs
Ser141	*	CK1, MAPKKK
Ser150	*	CK1,CK2,GRK,PKR
Ser154	*	CK1, DNA-PK, GRK, IKK, PKB
Thr156	*	ATM,CK1,PKB
Ser186	No	CK1, GSK3, IKK
Ser341	Yes	PAK, PKC
Ser396	Yes	MAPKKK, RAF1, S6K

(b)

Peptide	Sequence	Score	m/z	Charge
T14	GLTEDLGSNAGQGVK	70	763.4	2+
T15A	ESDVDSLTQGLK	52	685.9	2+
T15B	ESDVDSLTQGLK	29	685.9	2+
T15C	ESDVDSLTQGLK	44	685.9	2+
T15D	ESDVDSLTQGLK	16	511.1	3+
T16	GVNYGGDDSNPLSGQ EHQTISDEPK	32	908.8	3+
T17	SLPGQGNDLPQSHPSS EDEPK	46	767.1	3+
T29-30	GVFTKDYLSEK	72	683.8	2+
T30	DYLSEK	38	834.3	1+
T36	GAVGSLIGGGNK	55	555.4	2+

(d)

Figure 5. Identification of phosphorylation sites of CDeT11-24 by mass spectrometry (MS). (a) The sequence of CDeT11-24 (CAA05780) with the observed phosphorylation sites marked in green and red. (b) A table listing the phosphopeptide masses observed as well as phosphorylation models obtained from fragmentation. Sites marked in green represent models that best explain the majority of the tandem mass spectrometry (MS/MS) spectra collected for a given mass-to-charge ratio (m/z). The Mascot (Matrix Science, London, UK) scores reported here represent the best match for the given model relative to a fragmentation spectrum (a score above 16 indicates identity). Where an alternative model provided the best fit to at least one MS/MS spectrum, the highest score for that model is given. Alternative and equivocal phosphorylation sites are marked in red. The T16 phosphorylation site is tentative; the corresponding phosphopeptide was only observed in the strongest samples, and the resulting fragmentation was noisy, making interpretation difficult. (c) A table listing the high-certainty phosphorylation sites, their conservation between CDeT11-24 and its two closest homologs from *Arabidopsis thaliana* (RD29B, Q04980 and At4g255580/M7J2–50, Q8RY15), and the phosphorylation site models from group-based phosphorylation scoring (GPS) (http://973-proteinweb.ustc.edu.cn/gps/gps_web) which predict these sites with significant scores, and the Prosite pattern (http://www.expasy.org/prosite) matched by Ser341. Ser169 was omitted because of weak signal and lack of matching predictions. The asterisks mark those residues which are located in regions with low local homology. Abbreviations for kinase motifs: CK1, casein kinase I; DNA-PK, DNA-dependent protein kinase; GRK, G protein-coupled receptor kinase; GSK3, glycogen synthase kinase-3; IKK, I kappa-B kinase; MAPKKK, MAP kinase kinase kinase; PAK, p21-activated kinase; PKB, protein kinase B; RAF1, RAF proto-oncogene Ser/Thr-protein kinase 1; S6K, ribosomal protein S6 kinase; PKC, protein kinase C. (d) An example fragmentation spectrum of the phosphorylated T36 peptide. The sample was analysed with a high-capacity trap (HCTultra) ion trap mass spectrometer (Bruker Daltonics, Bremen, Germany).

Conservation of phosphorylation sites in homologs of CDeT11-24

Database searches showed that homology of CDeT11-24 to other plant proteins is restricted to particular stretches of the sequence. Residues 183–383 of CDeT11-24 comprise a conserved domain (Prodom entry PD010085) observed in six other plant proteins from tobacco (B57, Q8H0I1), spinach (CAP160, O50054) and *Arabidopsis* (At4g25580/ M7J2–50, Q8RY15; RD29A, Q06738 and RD29B, Q04980 and a purported kinase, Q9STE9). Three of these proteins (CAP160, RD29A and RD29B) are well-documented cold- and water-stress associated proteins (Kaye *et al.* 1998). Residues 226–252 of CDeT11-24 match the CAP160 repeat pattern (Interpro IPR012418) which appears three times in the CAP160 protein itself. Ser141, Ser150, Ser154 and

Ser186, and Thr156 all fall in a region of low homology between CDeT11-24 and its drought-stress-associated homologs, outside of the conserved domain or in regions of poor consensus. Ser341 clearly aligns to a Ser and a Thr in Swiss-Prot Q04980 and TrEMBL O65604, respectively, and Ser396 is strictly conserved. This phosphorylation site and the match to the sequence surrounding Ser341 fit the Prosite (http://www.expasy.org/prosite/) profile for phosphorylation by protein kinase C (Prosite pattern PS00005).

DISCUSSION

The results presented here suggest that phosphorylation and dephosphorylation of proteins are part of the desiccation tolerance mechanism of *C. plantagineum*. We show

that desiccation induces transient phosphorylation of the abundantly expressed dehydration-induced proteins CDeT11-24 and CDeT6-19 in leaves and roots. On the basis of sequence similarity, CDeT6-19 belongs to the group 2 LEA proteins or dehydrins, which are characterized by a Ser-rich sequence (S-segment) and one or more lysine-rich segments (Close 1996). The S-segment of the dehydrin Rab17 from maize can be phosphorylated by protein kinase casein kinase II (CK2) *in vitro* (Goday *et al*. 1994). It was recently demonstrated that all seven contiguous Ser residues are phosphorylated and that 5–7 mol of phosphate groups are incorporated into 1 mol of native protein (Jiang & Wang 2004). CDeT6-19 also contains an S-segment (RSGSSSSSSSE) which matches the S-segment consensus sequence (Svensson *et al*. 2002), followed by a consensus site for the protein kinase CK2 (Meggio, Marin & Pinna 1994). Furthermore, staining of polyacrylamide gels with phosphoprotein-specific stain resulted in very strong fluorescent signals for CDeT6-19. Because the intensity of this dye depends on the phosphorylation state of the protein, the high phosphoprotein signal compared to the amount of protein loaded onto the gel argues for multiple phosphorylation of CDeT6-19. In addition, treatment of this protein with CIP resulted in a pronounced shift into the basic pH during IEF, which can only be expected for proteins carrying more than one phosphate group.

Accumulation of CDeT6-19 was observed in both leaves and roots at an early stage after the onset of dehydration (90% RWC). The protein level decreased in leaves 4 d after rewatering of the plants, whereas in roots, the level does not change over the first 8 d and declines later in the resurrection process. Because the kinetics of phosphorylation perfectly matches those of the protein levels in both tissues, the phosphorylation of CDeT6-19 may be an important prerequisite for the function of this protein. Recent studies have shown that dehydrins are able to bind ions (Heyen *et al*. 2002; Kruger *et al*. 2002). It was also reported that dehydrins ERD14, ERD10 and COR47 are calcium-binding proteins. Phosphorylation of the corresponding S-segment is apparently responsible for the activation of ion binding (Alsheikh, Heyen & Randall 2003; Alsheikh, Svensson & Randall 2005). The authors proposed that these proteins may act as ionic buffers by sequestering calcium or other toxic ions to restrict the harmful effects of increasing ionic concentrations, or alternatively act as calcium-dependent chaperones. ERD14, ERD10 and COR47 proteins can be classified as acidic dehydrins. No calcium-binding activity was observed for the neutral maize dehydrin RAB18, although this protein carries an S-segment; thus, ion binding appears restricted to acidic dehydrins (Alsheikh *et al*. 2005). CDeT6-19 is a basic protein with a pI of 10.1; it therefore seems unlikely that ion binding is the primary biochemical function of CDeT6-19. A putative function of CDeT6-19 may be the protection of catalytic activities of enzymes. *In vitro* assays show that recombinant CDeT6-19 exhibited a protective activity on malate dehydrogenase or lactate dehydrogenase, when these enzymes were exposed to water loss (Reyes *et al*. 2005). The authors

speculated that the dehydrins exert their effect by binding to these enzymes, preventing conformational changes that would otherwise lead to inactivation. However, recombinant dehydrins that are not phosphorylated were used for these assays. Thus, phosphorylation of CDeT6-19 may enhance this effect or may determine the intracellular localization of the protein. Evidence that phosphorylation influences the intracellular localization has been described for the maize dehydrin Rab17 which is basic and thus resembles CDeT6-19 (Goday *et al*. 1994; Riera *et al*. 2004). Rab17 specifically interacts with the protein kinase subunit CK2β. Referring to a detailed analysis of the spatial distribution of Rab17 and CK2, the authors proposed that a corresponding Rab17/CK2β complex may be translocated to the nucleus, where CK2β associates with the CK2α subunit to generate the protein kinase holoenzyme. The resulting holoenzyme would then be able to phosphorylate Rab17, which may be the signal for the protein to be relocated to the cytoplasm, where it exerts its biological function (Riera *et al*. 2004).

In contrast to CDeT6-19, the other abundantly accumulating protein CDeT11-24 has not been classified to the established groups of LEA proteins. It was suggested that the CDeT11-24 protein is involved in sensing the water status of the plant (Velasco *et al*. 1998). This hypothesis is based on the finding that the CDeT11-24 protein is absent in untreated leaves, and the presence in roots is dependent on the culture conditions of the plants. CDeT11-24 was constitutively expressed in roots of plants grown in soil, whereas this protein was not detected when roots were kept in close contact with water (e.g. by cultivation in sterile agar). For our experiments, we have used only fully watered plants, so that CDeT11-24 was not detected in untreated roots and leaves. Upon dehydration, the protein transiently accumulated in both tissues like CDeT6-19, but phosphorylated CDeT11-24 was restricted to desiccated tissues.

Whole-protein MALDI-TOF analyses of phosphorylated CDeT11-24 indicated that most phosphoproteins carry only one phosphate group (data not shown). Yet several different tryptic phosphopeptides from CDeT11-24 were identified by LC-MS/MS, and fragmentation spectra indicated the possible phosphorylated Ser and Thr residues (Fig. 5). These observations indicate multiple independent phosphorylation sites. Sites which were best explained by the MS/MS spectra are Ser141, Ser154, Ser186, Ser341 and Ser396. Alternative and equivocal phosphorylation sites are Ser150, Thr156 and Ser169. Interestingly, the phosphorylation with the strongest signal (Ser341) occurs in the relatively well-conserved region containing the PD010085 domain (residues 183–383) (Fig. 6a). Residues 141, 150, 154, 156 and 169 fall in a region of low homology between CDeT11-24 and its dehydration-stress-associated homologs in spinach (CAP160) and *Arabidopsis* (RD29A and RD29B). Thus, the unique sequence in this region may be associated with a function above and beyond that of its homologs in less dehydration-resistant species. Interestingly, the proteins containing the conserved PD010085 domain also display a conserved lysine-rich pattern in their
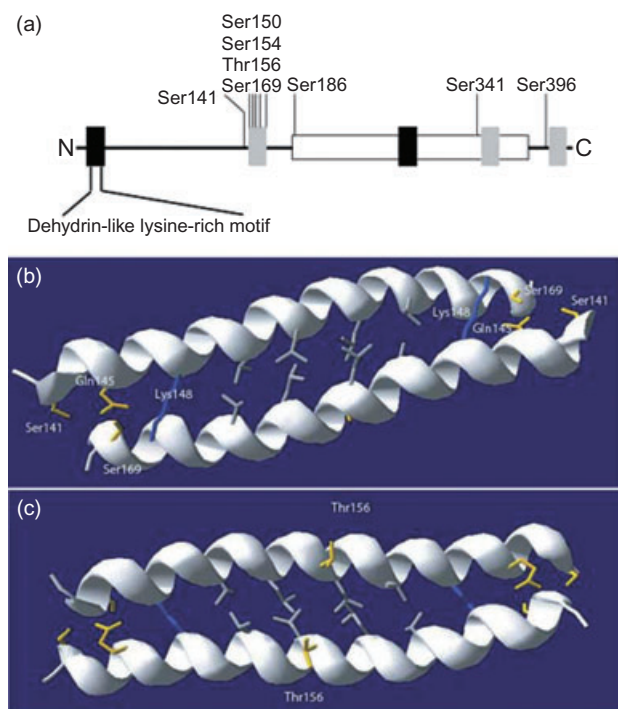
Figure 6. Schematic representation of the CDeT11-24 protein (a) and a model of phosphorylation-controlled dimerization (b, c). (a) The open box indicates the conserved domain (Prodom entry PD010085) and closed boxes show the positions of stretches with high coiled-coil probability (black) and lower coiled-coil probability (grey). The diagram shows the positions of phosphorylation sites and the lysine-rich motif, which contains the heptad repeat of hydrophobic side chains characteristic of coiled-coil regions. (b, c) Two views of a hypothetical model of an antiparallel coiled-coil dimerization domain in CDet11-24 encompassing residues 140–170. Both views reveal a hydrophobic core consisting of residues Val152, Leu155, Leu159 and Val162 which also occur in the canonical heptad repeat characteristic of a coiled coil. An antiparallel orientation was chosen on the basis of the presence of valine162 at a D position of the heptad repeat and on the possibility of favourable interactions formed by E-E′ pairs (Thr156-Thr156, Asn163-Glu149, Asn170-Asn142). (b) Illustration of the knob-and-hole interactions of Ser169 (knob) with a Ser141, Gln145 and Lys148 on both monomers. (c) The other side of the same model, illustrating the proximity of Thr156 residues on both molecules. A single phosphorylation, like those observed, at any of these three positions on either monomer, would strongly affect the affinity of such an interaction. Ser150 and Ser154 (not shown) are on the solvent-exposed face of the model, where phosphorylation could still affect binding, especially if higher ordered multimers form.

N-terminal regions which resembles the dehydrin lysine-rich motif.

Secondary structure predictions based on the hierarchical neural network (HNN) method (Guermeur *et al.* 1999) predict that CDeT11-24 and CDeT6-19 are 68 and 80% random coil, respectively, implying extended rather than globular conformations. This predicted lack of tertiary structure is consistent with previous nuclear magnetic resonance (NMR) studies of CDeT6-19, in which no stable structure could be discerned (Lisse *et al.* 1996). Coiled-coil

predictions (http://www.ch.embnet.org/software/COILS_form.html) performed on the CDeT11-24 primary sequence indicated two short stretches of relatively high coiled-coil probability (residues 10–50 and 271–284) (Fig. 6a). The first includes the dehydrin-like lysine-rich motif previously mentioned, which contains the canonical heptad repeat of hydrophobic side chains characteristic of a coiled coil (Mason & Arndt 2004). The pattern [AMLIV](2)-X-[KR]-[AMLIV]-[KR]-X-[KR]-[AMLIV]-[KR](2)-[AMLIV]-[KR]-X-X-[AM LIV] represents only the observed distribution of hydrophobic and positive residues. When used to search plant proteins in Swiss-Prot/TrEMBL (http://www.expasy.org/tools/scanprosite/), this pattern finds only those proteins containing the conserved C-terminal domain and two additional plant proteins (stress-related protein from *Brassica oleracea* – Q67BB3 – and hypothetical protein from rice – Q53RR4) which are homologs of CDeT11-24 on the basis of two-dimensional sequence similarity plots. Thus, this probable coiled-coil binding motif appears to be part of the function-defining architecture of CDeT11-24 and its analogs.

In addition, three stretches of lower coiled-coil probability are predicted which centred near residues 150, 350 and 400 (Fig. 6a). These regions may participate in lower affinity coiled-coil interactions and may coincide with the observed phosphorylations at residues 141, 150, 154, 156, 341 and 396 (Fig. 6a). Because phosphorylation has been proposed as a mechanism for influencing the stability and interactions of coiled-coil structures (Liang, Warrick & Spudich 1999; Steinmetz *et al.* 2001), the coincidence of the three regions with the observed CDeT11-24 phosphorylations becomes very interesting. The analogous phosphorylation site in RD29B (*Arabidopsis*) to Ser341 in CDeT11-24 (Fig. 5c) also coincides with the beginning of a segment of higher coiled-coil probability. In fact, nearly all proteins containing the PD010085 (Prodom) domain have a similar phosphorylatable residue in the immediate vicinity. If the function of phosphorylations in this region relates to influencing the stability of coiled-coil interactions, then precise alignment of phosphorylation sites among analogous proteins may not be essential for the function. CDeT11-24 might therefore form multiple sets of protein–protein interactions. The first set might involve the tight interaction of the higher probability coiled-coil regions. A second set would involve interaction between lower probability coiled-coil regions which could be modified by phosphorylation. Phosphorylation is known to either disrupt (Steinmetz *et al.* 2001) or induce (Liang *et al.* 1999) coiled-coil structures. Figure 6 provides a model of how phosphorylation might control the dimerization of the CDeT11-24 protein.

The presence of multiple coiled-coil interaction domains in CDeT11-24 could provide a mechanism for regulated protein oligomerization. Thus, similar to what Goyal *et al.* (2003) propose in the case of AavLEA, CDeT11-24's various coiled coils, possibly in combination with those of other dehydrins, could create a stabilizing protein network. These structures could provide protection during the initial stages

of dehydration. Phosphorylation could alter the interactions forming these structures as dehydration progresses and other protection mechanisms begin to act, for example, the accumulation of sucrose. Though phosphorylation occurs at several different sites of CDeT11-24 during dehydration, we propose that these diverse phosphorylations may regulate similar intermolecular interactions by the same mechanism.

In conclusion, we show for the first time the dehydration-induced transient phosphorylation of two abundant desiccation-responsive proteins in leaves and roots of *C. plantagineum*. We would like to suggest that CDeT11-24 contributes to the plant's desiccation tolerance in a process, based on coiled-coil interactions with itself and possibly with other proteins such as dehydrins. The observed phosphorylation of CDeT11-24 late in dehydration could alter the stability or specificity of these interactions, thus regulating this protective mechanism.

ACKNOWLEDGMENTS

REFERENCES

Alsheikh M.K., Heyen B.J. & Randall S.K. (2003) Ion-binding properties of the dehydrin ERD14 are dependent upon phosphorylation. *Journal of Biological Chemistry* **278**, 40882–40889.

Alsheikh M.K., Svensson J.T. & Randall S.K. (2005) Phosphorylation regulated ion-binding is a property shared by the acidic subclass dehydrins. *Plant, Cell & Environment* **28**, 1114–1122.

Bartels D. (2005) Desiccation tolerance studied in the resurrection plant *Craterostigma plantagineum*. *Integrative and Comparative Biology* **45**, 696–701.

Bartels D. & Salamini F. (2001) Desiccation tolerance in the resurrection plant *Craterostigma plantagineum*. A contribution to the study of drought tolerance at the molecular level. *Plant Physiology* **127**, 1346–1353.

Bartels D. & Sunkar R. (2005) Drought and salt tolerance in plants. *Critical Reviews in Plant Sciences* **24**, 23–58.

Bernacchia G., Schwall G., Lottspeich F., Salamini F. & Bartels D. (1995) The transketolase gene family of the resurrection plant *Craterostigma plantagineum*: differential expression during the rehydration phase. *EMBO Journal* **14**, 610–618.

Close T.J. (1996) Dehydrins: emergence of a biochemical role of a family of plant dehydration proteins. *Physiologia Plantarum* **97**, 795–803.

Cuming A. (1999) LEA proteins. In *Seed Proteins* (eds P.R. Shewry & R. Casey) pp. 753–780. Kluwer Academic Publisher, Dordrecht, the Netherlands.

Fengfeng Z., Yu X., Guoliang C. & Xuebiao Y. (2004) GPS: a novel group-based phosphorylation predicting and scoring method. *Biochemical and Biophysical Research Communications* **325**, 1443–1448.

Gaff D.F. (1971) Desiccation-tolerant flowering plants in Southern Africa. *Science* **174**, 1033–1034.

Goday A., Sánchez-Martínez D., Gómez J., Puigdomènech P. & Pagès M. (1988) Gene expression in developing *Zea mays* embryos. Regulation by abscisic acid of a highly phosphorylated 23- to 25-kD group of proteins. *Plant Physiology* **88**, 564–569.

Goday A., Jensen A.B., Culianez-Macià F.B., Albà M.M., Figueras M., Serratosa J., Torrent M. & Pagès M. (1994) The maize abscisic acid-responsive protein Rab17 is located in the nucleus and interacts with nuclear localization signals. *Plant Cell* **6**, 351–360.

Goyal K., Tisi L., Basran A., Browne J., Burnell A., Zurdo J. & Tunnacliffe A. (2003) Transition from natively unfolded to folded state induced by desiccation in an anhydrobiotic nematode protein. *Journal of Biological Chemistry* **278**, 12977–12984.

Goyal K., Walton L.J. & Tunnacliffe A. (2005) LEA proteins prevent protein aggregation due to water stress. *Biochemical Journal* **388**, 151–157.

Guermeur Y., Geourjon C., Gallinari P. & Deleage G. (1999) Improved performance in protein secondary structure prediction by inhomogeneous score combination. *Bioinformatics* **15**, 413–421.

Guy C.L. & Haskell D. (1989) Preliminary characterization of high molecular mass proteins associated with cold acclimation in spinach. *Plant Physiology and Biochemistry* **27**, 777–784.

Heyen B.J., Alsheikh M.K., Smith E.A., Torvik C.F., Seals D.F. & Randall S.K. (2002) The calcium-binding activity of a vacuole-associated, dehydrin like activity is regulated by phosphorylation. *Plant Physiology* **47**, 675–687.

Huber S.C. & Hardin S.C. (2004) Numerous posttranslational modifications provide opportunities for the intricate regulation of metabolic enzymes at multiple levels. *Current Opinion in Plant Biology* **7**, 319–322.

Jiang X. & Wang Y. (2004) β-elimination coupled with tandem mass spectrometry for the identification of *in vivo* and *in vitro* phosphorylation sites in maize dehydrin DHN1 protein. *Biochemistry* **43**, 15567–15576.

John M., Schmidt J., Wieneke U., Kondorosi E., Kondorosi A. & Schell J. (1985) Expression of the nodulation gene nod C of *Rhizobium meliloti* in *Escherichia coli*: role of the nod C gene product in nodulation. *EMBO Journal* **4**, 2425–2430.

Kaye C., Neven L., Hofig A., Li Q.B., Haskell D. & Guy C. (1998) Characterization of a gene for spinach CAP160 and expression of two spinach cold-acclimation proteins in tobacco. *Plant Physiology* **116**, 1367–1377.

Kruger C., Berkowitz O., Stephan U.W. & Hell R. (2002) A metal-binding member of the late embryogenesis abundant protein family transports iron into the phloem of *Ricinus communis* L. *Journal of Biological Chemistry* **277**, 25062–25069.

Laemmli (1970) Cleavage of structural proteins during the assembly of the head of maize bacteriophage T4. *Nature* **227**, 680–685.

Liang W., Warrick H.M. & Spudich J.A. (1999) A structural model for phosphorylation control of *Dictyostelium* myosin II thick filament assembly. *Journal of Cell Biology* **147**, 1039–1048.

Lisse T., Bartels D., Kalbitzer H.R. & Jaenicke R. (1996) The recombinant dehydrin-like desiccation stress protein from the resurrection plant *Craterostigma plantagineum* displays no defined three-dimensional structure in its native state. *Biological Chemistry* **377**, 555–561.

Makrantoni V., Antrobus R., Botting C.H. & Coote P.J. (2005) Rapid enrichment and analysis of yeast phosphoproteins using affinity chromatography, 2D-PAGE and peptide mass fingerprinting. *Yeast* **22**, 401–414.

Mason J.M. & Arndt K.M. (2004) Coiled coil domains: stability, specificity, and biological implications. *Chembiochem* **5**, 170–176.

Meggio F., Marin O. & Pinna L.A. (1994) Substrate specificity of protein kinase CK2. *Cellular and Molecular Biology Research* **40,** 401–409.

Metodiev M.V., Timanova A. & Stone D.E. (2004) Differential phosphoproteome profiling by affinity capture and tandem matrix-assisted laser desorption/ionization mass spectrometry. *Proteomics* **4,** 1433–1438.

Pawson T. & Scott J.D. (2005) Protein phosphorylation in signaling – 50 years and counting. *Trends in Biochemical Sciences* **30,** 286–290.

Reyes J.L., Rodrigo M.-J., Colmenero-Flores J.M., Gil J.-V., Garay-Arroyo A., Campos F., Salamini F., Bartels D. & Covarrubias A.A. (2005) Hydrophilins from distant organisms can protect enzymatic activities from water limitation effects *in vitro*. *Plant, Cell & Environment* **28,** 709–718.

Riera M., Figueras M., López C., Goday A. & Pagès M. (2004) Protein kinase CK2 modulates developmental functions of the abscisic acid responsive protein Rab17 from maize. *Proceedings of the National Academy of Sciences of the USA* **101,** 9879–9884.

Saavedra L., Svensson J., Carballo V., Izmendi D., Welin B. & Vidal S. (2006) A dehydrin gene in *Physcomitrella patens* is required for salt and osmotic stress tolerance. *Plant Journal* **45,** 237–249.

Schneider K., Wells B., Schmelzer E., Salamini F. & Bartels D. (1993) Desiccation leads to a rapid accumulation of both cytosolic and chloroplastic proteins in the resurrection plant *Craterostigma plantagineum*. *Planta* **189,** 120–131.

Shevchenko A., Wilm M., Vorm O. & Mann M. (1996) Mass spectrometric sequencing of proteins from silver stained polyacrylamide gels. *Analytical Chemistry* **68,** 850–858.

Steinmetz M.O., Jahnke W., Towbin H., García-Echeverría C., Voshol H., Müller D. & van Oostrum J. (2001) Phosphorylation disrupts the central helix in Op18/stathmin and suppresses binding to tubulin. *EMBO Reports* **2,** 505–510.

Svensson J., Ismail A.M., Palva E.T. & Close T.J. (2002) Dehydrins. In *Cell and Molecular Responses to Stress: Sensing, Signaling and Cell Adaption* (eds K.B. Storey & J. M. Storey) pp. 155–171. Elsevier Press, Amsterdam, the Netherlands.

Towbin H., Staehelin T. & Gordon J. (1979) Electrophoretic transfer of proteins to nitrocellulose sheets: procedure and some applications. *Proceedings of the National Academy of Sciences of the USA* **76,** 4350–4354.

Velasco R., Salamini F. & Bartels D. (1998) Gene structure and expression analysis of the drought-induced and abscisic acid-responsive CDeT11-24 gene family from the resurrection plant *Craterostigma plantagineum* Hochst. *Planta* **204,** 459–471.

Wang W., Scali M., Vignani R., Spadafora A., Sensi E., Mazzuca S. & Cresti M. (2003) Protein extraction for two-dimensional electrophoresis from olive leaf, a plant tissue containing high levels of interfering compounds. *Electrophoresis* **24,** 2369–2375.

Wise M.J. & Tunnacliffe A. (2004) POPP the question: what do LEA proteins do? *Trends in Plant Science* **9,** 13–17.